Published in final edited form as:
J Neurosci Methods. 2011 July 15; 199(1): 10–14. doi:10.1016/j.jneumeth.2011.04.011.

Murine diffusion imaging using snapshot interleaved EPI acquisition at 7 Tesla

David N. Guilfoyle[*], **Scott Gerum**, and **Jan Hrabe**
Center for Advanced Brain Imaging, Nathan S. Kline Institute for Psychiatric Research, 140 Old Orangeburg Road, Orangeburg, 10962, New York, USA.

Abstract

Diffusion Tensor Imaging (DTI) is a powerful magnetic resonance imaging tool for quantitative assessment of white matter micro structure. The majority of DTI methods employ Echo Planar Imaging (EPI) because it is insensitive to motion. However, EPI suffers from distortions and signal losses induced by inhomogeneities in magnetic field susceptibility. This is particularly accentuated in murine imaging at very high magnetic fields. The purpose of this study is to demonstrate that a Snapshot Interleaved EPI acquisition block combined with a stimulated echo module for diffusion sensitization can be successfully used to obtain high quality DTI of a mouse brain at 7 Tesla. This technique preserves the EPI speed but reduces its susceptibility artifacts and signal losses. Signal to noise ratio is also reduced but remains higher than in the DTI acquisitions based on a fast low angle shot technique. In vivo results using this new approach are presented along with a full description of the methodology.

Keywords

Diffusion Tensor Imaging; fractional anisotropy; white matter; mouse brain

1. Introduction

In recent years, magnetic resonance diffusion tensor imaging (DTI) (Basser et al., 1994a; Basser et al., 1994b) has emerged as a unique tool for the noninvasive study and characterization of white matter microstructure. Historically, rats have most often been used in models of various diseases but with advent of transgenic mouse models, there is a growing body of literature citing the use of DTI in murine applications. Unfortunately, DTI of a mouse brain is technically very difficult. Inhomogeneities and discontinuities in bulk magnetic susceptibility cause local magnetic field gradients, which result in distortions and signal losses in any technique sensitive to the T_2^* relaxation effects. The mouse brain is very small and has to be imaged at high field strengths, typically more than 4 Tesla, to achieve sufficient signal to noise ratio (SNR) for the sub-millimeter image resolutions typically required. The bulk susceptibility effects scale linearly with the main field strength, making the high field imaging particularly vulnerable. Furthermore, the mouse brain exhibits a large surface to volume ratio, much greater than a rat or a human brain (Grieve et al., 2000).

[*]Corresponding Author: Tel. 845 398 5573, dguilfoyle@nki.rfmh.org.

Because the brain surface represents a major source of the locally generated field gradients, a significantly larger percentage of a mouse brain is affected.

The most common DTI approach in larger animals and humans is based on Echo Planar Imaging (EPI). This is not the case for in vivo mouse brain imaging. A traditional Pulse Gradient Spin Echo (PGSE) sequence (Taylor and Bushell, 1985) seems to be the most prevalent in literature (Basser et al., 1994a; Harsan et al., 2007; Mayer et al., 2007; Larvaron et al., 2007; Assaf et al., 2008), sometimes supplemented with respiratory gating (Boska et al., 2007; Hui et al., 2008). Although the SNR is high, this method is very prone to motion induced errors and requires long scan times. However, it is very suitable for diffusion measurements in vitro (Guilfoyle et al., 2003).

Other reported murine DTI techniques have employed radial Fast Spin Echo (FSE) (Ahmad et al., 2005) and conventionally segmented EPI with each segment separated by a long repetition time from the next (Assaf et al., 2008). Acquisition times are much shorter than in the PGSE but both techniques are sensitive to motion induced phase errors. The implementation of FSE is further complicated by the diffusion gradients around the first refocusing pulse which violate the Carr-Purcell-Meiboom-Gill condition for spin echo formation and cause phase inconsistencies between the spin echoes and the stimulated echoes. This problem has been addressed in several studies (Williams et al., 1999; Norris and Driesel, 2001) and diffusion sequences based on FSE are still of great interest but they are not commonly employed in murine DTI.

To the best of our knowledge, there have only been two DTI studies of in-vivo mouse brain using a snapshot technique (Boretius et al., 2004; Boretius et al., 2007). Both employed diffusion sensitization based on a stimulated echo, followed by a Fast Low Angle Shot (FLASH) acquisition block. Although the FLASH acquisition is essentially distortion free, the disadvantage of this method is its low SNR due to the low flip angles necessary for high speed FLASH imaging.

EPI is the imaging modality typically used for DTI studies in larger animals and humans because of its short acquisition time and reduced sensitivity to motion. However, EPI is very sensitive to magnetic field susceptibility effects and the DTI of a mouse brain with EPI acquisition module is therefore particularly challenging. We have previously shown that the Snapshot Interleaved EPI (SIEPI) (Guilfoyle and Hrabe, 2006) can significantly reduce susceptibility artifacts associated with murine EPI acquisition. The purpose of this study is to demonstrate that the SIEPI acquisition block preceded by a stimulated echo module for diffusion sensitization can be readily used to obtain high quality DTI of a mouse brain. The interleaved EPI segments are executed in immediate succession to preserve the snapshot capability of EPI. This is an important feature for diffusion measurements because acquisition of each segment in a separate repetition period is prone to severe phase errors.

Diffusion sensitized SIEPI achieves higher SNR than the methods based on FLASH. They preserve the snapshot character of the EPI but reduce susceptibility artifacts pronounced in the traditional EPI method. An optimum balance between the properties of a traditional EPI and the FLASH techniques can be established by altering the number of SIEPI segments from one (the EPI limit) up to to the full phase encode resolution (the FLASH limit). The work reported here is the first using a snapshot technique based on EPI to perform the DTI of a mouse brain in vivo.

2. Materials and Methods

2.1 The diffusion weighted SIEPI sequence

The sequence diagram is shown in Figure 1. Diffusion preparation is achieved in the first part of a stimulated echo module. This module starts with a conventional PGSE combination of excitation and refocusing RF pulses, which is conceptually equivalent to the first RF pulse in a conventional stimulated echo sequence except for the transverse magnetization being modified by a pair of the diffusion encoding gradients placed symmetrically around the PGSE refocusing pulse. The next RF pulse stores the diffusion encoded transverse magnetization into the longitudinal direction. Any remaining transverse magnetization is destroyed by spoiler gradients during the subsequent mixing time. The variable flip angle RF pulses of the SIEPI acquisition module then sample the stored magnetization. They are designed to extract equal amounts of transverse magnetization after every pulse. The SIEPI pulses thus collectively serve in a manner similar to the third 90 degree RF pulse in a conventional stimulated echo sequence, converting all the available stored magnetization into a useful signal. The example in Figure 1 shows 3 SIEPI pulses, each followed by the corresponding acquisition segment. These excitation-acquisition segments are applied in immediate succession. The total echo time is composed from the TE_{PGSE} component governed by the desired diffusion time Δ, and from the TE_{STIM} component governed by the length of a single acquisition segment T_{α}.

The SIEPI acquisition module has been described in details previously (Guilfoyle and Hrabe, 2006). Briefly, there are four key elements: 1) Variable flip angles $\alpha_s = \sin^{-1}(1/\sqrt{(n-s)})$, $s = 0, 1, 2, \ldots, n-1$ are employed to equalize the transverse magnetization among all n segments. 2) Polarity of the read gradient is reversed between the segments to preserve the k-space structure of a traditional EPI in the dataset combined from all interleaved segments. 3) Onset of acquisition in a segment s is delayed by $(s/n)\ T_{RL}$ to ensure smooth T_2^* decay over the k-space data set, free of a step-wise modulation and the associated ghosting in the reconstructed image. 4) There are no other delays between the acquisition blocks to avoid any loss of temporal resolution in comparison with the conventional EPI.

In order to assess the optimum combination of a number of segments n and acquisition bandwidth BW, we modeled the signal to noise ratio (SNR) as a function of these two parameters using Mathematica (Wolfram Research, Champaign, IL, USA). Other model parameters reflected typical values found in mouse brain imaging (T_1 = 1.6 s, T_2 = 38 ms, T_2^* = 15 ms, TE_{PGSE} = 20 ms, T_{MIX} = 10 ms, acquisition matrix 64 × 64, $b\ D$ = 1.0). The number of segments was varied from 1 to 64 and the acquisition bandwidth from 20 to 200 kHz. We also tested the FLASH-like acquisition (n = 64) with a constant flip angle of 12 degrees and eliminated onset delays, in agreement with the sequence used by Boretius et al. (2006).

2.2 Animals

Six male C57BL/6 mice with an average age of 5 months and an average weight of 30 g were used in this study. The animals were anesthetized with a mixture of isoflurane (2%), NO_2 (75%), and O_2 (23%). For the anesthesia maintenance, isoflurane concentration was reduced to 1%, with a slight correction for individual body weight. After being anesthetized, the mice were positioned in a custom head holder designed to fit inside the imaging coil. The holder had a plastic bite bar on which the front teeth were secured in order to minimize movement during the imaging session. The chest and abdomen of the animal remained outside of the RF coil. Body temperature was maintained with warm air circulated by a Bair Hugger 500 patient warming system (Augustine Medical Inc., Eden Prairie, MN, USA). The

temperature was monitored with a rectal probe and remained at 37 ± 0.5 °C throughout the experiment.

All animal procedures were in accordance with National Institutes of Health guidelines and were approved by the Institutional Animal Care and Use Committee of the Nathan S. Kline Institute for psychiatric research.

2.3 Imaging

All the data were obtained on a 7.0 T Magnetic Resonance Research Systems console (formerly SMIS, Guildford, U.K.) attached to a 40 cm bore magnet (Magnex Scientific, Yarnton, U.K.). The gradient coil insert with internal diameter of 10 cm had a maximum gradient strength of 500 mT/m and a minimum rise time of 250 μs. A 6 cm ID quadrature birdcage coil (Nova Medical, Wilmington, MA, USA) was used for RF transmission, and a 1 cm single loop surface coil for signal reception.

All diffusion-weighted images were acquired with the following parameters: matrix size 64 × 64 zero-filled to 128 × 128 before reconstruction, FOV 15 mm, 11 contiguous transverse slices 1 mm thick, acquisition bandwidth 200 kHz, 64 repetitions lasting 30 min., *TR* 4 s, *TE* 35 ms, TE_{STIM} 15 ms, TE_{PGSE} 20 ms, T_{RL} 0.5 ms, 3 excitation-acquisition segments with flip angles 35°, 45°, and 90°. The diffusion gradients lasted 4 ms and were placed 10 ms apart, producing a *b*-value of 953 s/mm^2. Diffusion was measured along 6 non-collinear gradient directions: (G_{read}, G_{phase}, G_{slice}) = [(1,1,0), (0,1,1), (1,0,1), (−1,1,0), (0,−1,1), (1,0,−1)], and also with no diffusion gradients. The gradient spoilers had an amplitude of 200 mT/m and lasted for 2 ms.

Fractional anisotropy index (FA, Basser et al., 1996) was used to evaluate a degree of diffusion anisotropy, calculated and displayed on a voxel by voxel basis. The FA is independent of the orientation of diffusion in the voxel but reflects deviation from isotropic diffusion ranging from 0 (perfectly isotropic diffusion) to 1 (diffusion movement restricted to a single direction). Directional information was incorporated by color coding the scalar FA map with the red, green and blue colors to signify the left—right, ventral—dorsal, and caudal—rostral directions, respectively (Pajevic et al., 1999). In this way, both the gray scale and the color coded FA maps were generated for all acquired diffusion data.

T_2 weighted spin echo images (*TR* 4 s, *TE* 35 ms) were acquired to show the underlying anatomy with higher resolution. These images had the same FOV geometry as the diffusion images but the matrix size was 256 × 256.

3. Results

Figure 2 shows a typical series of 5 consecutive images from a multi slice data set. The first row (a) shows the SIEPI images acquired with with $b = 0$ s/mm^2. The next six rows (b—g) show the diffusion weighted images ($b = 953$ s/mm^2) acquired along six non-collinear spatial directions. Row (h) contains the corresponding FA maps, and row (i) shows these maps directionally color coded. The bottom row (j) displays higher resolution anatomical spin echo images.

The average SNR of the central image without diffusion weighting is 113. This value was obtained from the mean signal intensity of the magnitude image divided by $\sqrt{(2-\pi/2)}\,\sigma$, where σ is the standard deviation of the pixel intensities in a background region not affected by ghosting. Boretius et al. (2007) reported the SNR of 18 for the real image obtained with the FLASH half Fourier method (Boretius et al., 2007). However, the two acquisitions

differed in several imaging parameters relevant for SNR, making a direct comparison difficult.

Table 1 summarizes the SNR and FA measurements from 6 animals in a gray matter cortical region and in a white matter region of corpus callosum. The contrast to noise ratio between these two regions was 46 ± 6 (mean ± SD). The obtained FA values are in close agreement with other published values in rodents (Boretius et al., 2007; Nair et al., 2005; Hui et al., 2008).

Figure 3 documents the reproducibility of the SIEPI based technique. It shows the non diffusion weighted image from a similarly positioned slice in the other animals used in this study. The associated color coded FA maps are also depicted.

A mathematical model provides some insight into the SNR behavior of the SIEPI based DTI sequence. Figure 4 shows that the highest SNR can be expected when a low number (1—5) of segments is acquired at high bandwidth (150—250 kHz). This closely resembles the parameters chosen in this study. The region where many segments are scanned at low bandwidth represents the FLASH-like acquisition, where the SNR is also relatively high. In practice, the minimum number of SIEPI segments is given by the degree of acceptable distortions and the quality of shimming. When much shorter T_2^* is used in the model, the area of the maximum SNR shifts towards higher number of segments, as would be expected (data not shown). On the other hand, the minimum bandwidth desirable for the FLASH-like acquisition is limited by the T_1 effect on the point spread function. With model parameters closely resembling the SIEPI acquisition used in this study and in the FLASH acquisition used by Boretius et al. (2007), the model estimates that the SIEPI SNR is higher by approximately 30—50%, depending on T_1.

We have also performed simulations of the imaging efficiency, defined as the SNR normalized to a square root of total imaging time (Johnson et al., 1999). If only a single acquisition is made, the SIEPI is about 3.4 times more efficient due to its much shorter acquisition time. However, this is not a typical situation. Many different acquisitions with various diffusion directions or *b*-values are usually obtained. Because the longitudinal magnetization must be allowed to substantially recover from its saturated state after each acquisition, the overall repetition time is much longer than the acquisition time and governs the total imaging time. The advantage of SIEPI based sequence in terms of imaging efficiency is then almost identical to the advantage in SNR, about 30—50%. However, SIEPI can acquire approximately 5 times more slices within the same repetition period.

4. Discussion

We have demonstrated that the SIEPI acquisition combined with a stimulated echo diffusion preparation offers a simple and robust method for DTI in a mouse brain in vivo at 7.0 Tesla. The method appreciably reduces the susceptibility related deformations and signal losses while preserving the high temporal resolution and the snapshot capability of the conventional EPI. This is important for diffusion measurements which are very sensitive to motion induced artifacts. Any experiment which divides the image acquisition into several segments with their own individual diffusion encodings will likely introduce significant motion induced phase errors. Although respiratory gating can to some extent reduce these errors, it increases the total acquisition time depending on the respiration rate of the animal and the minimum TR required to eliminate the steady state effects.

Surprisingly, there have been only two other reports of single shot DTI measurements in a mouse brain in vivo (Boretius et al., 2004; Boretius et al., 2007), both using a FLASH sequence for the acquisition block. Although it is virtually distortion-free, the main

disadvantages of the FLASH based technique are its lower SNR and longer acquisition time per slice. Several modifications have been implemented to address this problem. Implementation of half Fourier phase-encoding scheme with increased flip angle increases SNR without sacrificing spatial resolution of the original full *k*-space FLASH image acquired in a center-out fashion (Finsterbusch and Frahm, 2002). However, the SNR and acquisition speed remain significantly lower than in EPI-based methods.

One limitation of SIEPI based sequences results from the necessity to obtain identical amount of transverse magnetization in each segment. A primary source of variations in the transverse magnetization is the T_1 relaxation process. If the T_1 relaxation was rapid, the flip angle series would become suboptimal, resulting in sudden signal steps in the *k*-space and thus to appearance of $n - 1$ ghosts. However, our simulations showed that with typical high bandwidth and low number of segments, the T_1 would have to be shorter than 0.5 s for the ghosting level to reach 1%. For a mouse brain at 7 Tesla, typical T_1 values are 1.8 s in gray matter and 1.5 s in white matter (Guilfoyle et al., 2003).

In conclusion, SIEPI with stimulated echo is a robust DTI method with fairly straightforward implementation where the desired compromise between the SNR and distortions can be adjusted by altering the number of segments.

Acknowledgments

This work was supported by the National Institute of Aging (P01 AG017617 to R. Nixon).

References

Ahmad I, Lope-Piedrafita S, Bi X, Hicks C, Yao Y, Yu C, Chaitkin E, Howison CM, Weberg L, Trouard TP, Erickson RP. Allopregnanolone treatment, both as a single injection or repetitively, delays demyelination and enhances survival of Niemann-Pick C mice. J Neurosci Res. 2005; 82:811–821. [PubMed: 16273542]

Assaf Y, Galron R, Shapira I, Nitzan A, Blumenfeld-Katzir T, Solomon AS, Holdengreber V, Wang ZQ, Shiloh Y, Barzilai A. MRI evidence of white matter damage in a mouse model of Nijmegen breakage syndrome. Exp Neurol. 2008; 209:181–191. [PubMed: 17976584]

Basser PJ, Mattiello J, LeBihan D. Estimation of the effective self-diffusion tensor from the NMR spin echo. J Magn Reson B. 1994a; 103:247–254. [PubMed: 8019776]

Basser PJ, Mattiello J, LeBihan D. MR diffusion tensor spectroscopy and imaging. Biophys J. 1994b; 66:259–267. [PubMed: 8130344]

Boretius S, Natt O, Watanabe T, Tammer R, Ehrenreich L, Frahm J, Michaelis T. In vivo diffusion tensor mapping of the brain of squirrel monkey, rat, and mouse using single-shot STEAM MRI. Magma. 2004; 17:339–347. [PubMed: 15580374]

Boretius S, Wurfel J, Zipp F, Frahm J, Michaelis T. High-field diffusion tensor imaging of mouse brain in vivo using single-shot STEAM MRI. J Neurosci Methods. 2007; 161:112–117. [PubMed: 17174402]

Boska MD, Hasan KM, Kibuule D, Banerjee R, McIntyre E, Nelson JA, Hahn T, Gendelman HE, Mosley RL. Quantitative diffusion tensor imaging detects dopaminergic neuronal degeneration in a murine model of Parkinson's disease. Neurobiol Dis. 2007; 26:590–596. [PubMed: 17428671]

Finsterbusch J, Frahm J. Half Fourier Single Shot STEAM MRI. Magn Reson Med. 2002; 47:611–615. [PubMed: 11870850]

Grieve SM, Blamire AM, Styles P. The effect of bulk susceptibility on murine snapshot imaging at 7.0 T: a comparison of snapshot imaging techniques. Magn Reson Med. 2000; 43:747–755. [PubMed: 10800041]

Guilfoyle DN, Helpern JA, Lim KO. Diffusion tensor imaging in fixed brain tissue at 7.0 T. NMR Biomed. 2003; 16:77–81. [PubMed: 12730948]

Guilfoyle DN, Dyakin VV, O'Shea J, Pell GS, Helpern JA. Quantitative measurements of proton spin-lattice (T1) and spin-spin (T2) relaxation times in the mouse brain at 7.0 T. Magn Reson Med. 2003; 49:576–580. [PubMed: 12594763]

Guilfoyle DN, Hrabe J. Interleaved snapshot echo planar imaging of mouse brain at 7.0 T. NMR Biomed. 2006; 19:108–115. [PubMed: 16411168]

Harsan LA, Poulet P, Guignard B, Parizel N, Skoff RP, Ghandour MS. Astrocytic hypertrophy in dysmyelination influences the diffusion anisotropy of white matter. J Neurosci Res. 2007; 85:935–944. [PubMed: 17278151]

Hui ES, Cheung MM, Qi L, Wu EX. Towards better MR characterization of neural tissues using directional diffusion kurtosis analysis. Neuroimage. 2008; 42:122–134. [PubMed: 18524628]

Johnson G, Wadghiri YZ, Turnbull DH. 2D and 3D MRI sequences are often equally sensitive. Magn Reson Med. 1999; 41:824–828. [PubMed: 10332860]

Larvaron P, Boespflug-Tanguy O, Renou JP, Bonny JM. In vivo analysis of the post-natal development of normal mouse brain by DTI. NMR Biomed. 2007; 20:413–421. [PubMed: 17120295]

Mayer D, Zahr NM, Adalsteinsson E, Rutt B, Sullivan EV, Pfefferbaum A. In vivo fiber tracking in the rat brain on a clinical 3T MRI system using a high strength insert gradient coil. Neuroimage. 2007; 35:1077–1085. [PubMed: 17331742]

Nair G, Tanahashi Y, Low PH, Billings-Gagliardi S, Schwartz WJ, Duong TQ. Myelination and long diffusion times alter diffusion-tensor-imaging contrast in myelin-deficient shiverer mice. Neuroimage. 2005; 28:165–174. [PubMed: 16023870]

Norris DG, Driesel W. Online motion correction for diffusion-weighted imaging using navigator echoes: Application to RARE imaging without sensitivity loss. Magn Reson Med. 2001; 45:729–733. [PubMed: 11323797]

Pajevic S, Pierpaoli C. Color schemes to represent the orientation of anisotropic tissues from diffusion tensor data: Applications to white matter fiber tract mapping in the human brain. Magn Reson Med. 1999; 42:526–540. [PubMed: 10467297]

Taylor DG, Bushell MC. The spatial mapping of translational diffusion coefficients by the NMR imaging technique. Phys Med Biol. 1985; 30:345–349. [PubMed: 4001161]

Williams CF, Redpath TW, Norris DG. A novel fast split-echo multi-shot diffusion-weighted MRI method using navigator echoes. Magn Reson Med. 1999; 41:734–742. [PubMed: 10332849]

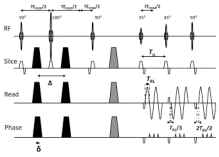

Figure 1.

Pulse sequence diagram for diffusion sensitized Snapshot Interleaved EPI (SIEPI). The stimulated echo module achieves diffusion sensitization with diffusion time Δ and gradient duration δ. The spin echo component has an echo time of TE_{PGSE} and the stimulated echo component has an echo time of TE_{STIM}. The echo spacing is given by T_{RL} and the duration of each segment is T_{σ}.

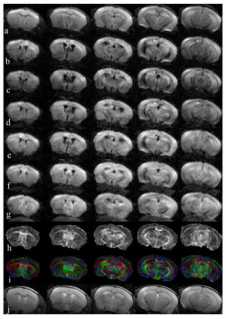

Figure 2.
Typical data set from a series of 5 consecutive slices. Each column corresponds to a single slice. Row (a) shows the SIEPI images acquired with $b = 0$ s/mm^2. Rows (b) through (g) represent the diffusion weighted images with spatial orientations of the diffusion gradients (G_{read}, G_{phase}, G_{slice}) = (1,1,0), (0,1,1), (1,0,1), (−1,1,0), (0,−1,1), (1,0,−1), respectively. Rows (h) and (i) show the gray scale and color coded FA maps with left—right (readout) diffusion direction red, ventral—dorsal (phase) direction green and caudal—rostral (slice) direction blue. Row (j) displays the corresponding high resolution anatomical maps.

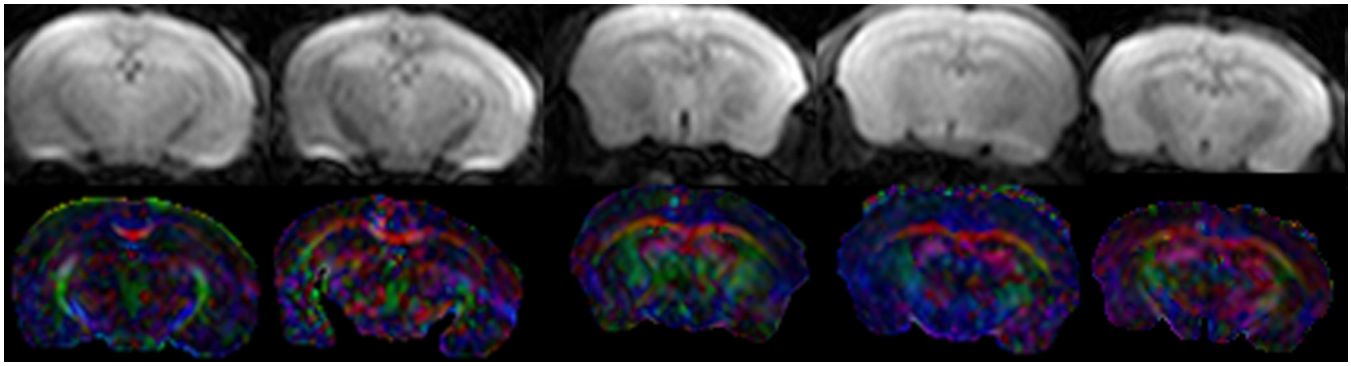

Figure 3.
The images acquired without diffusion weighting and the associated color coded FA maps from five different animals demonstrate reproducibility of the acquisition. Each column represents a similarly positioned slice in each mouse.

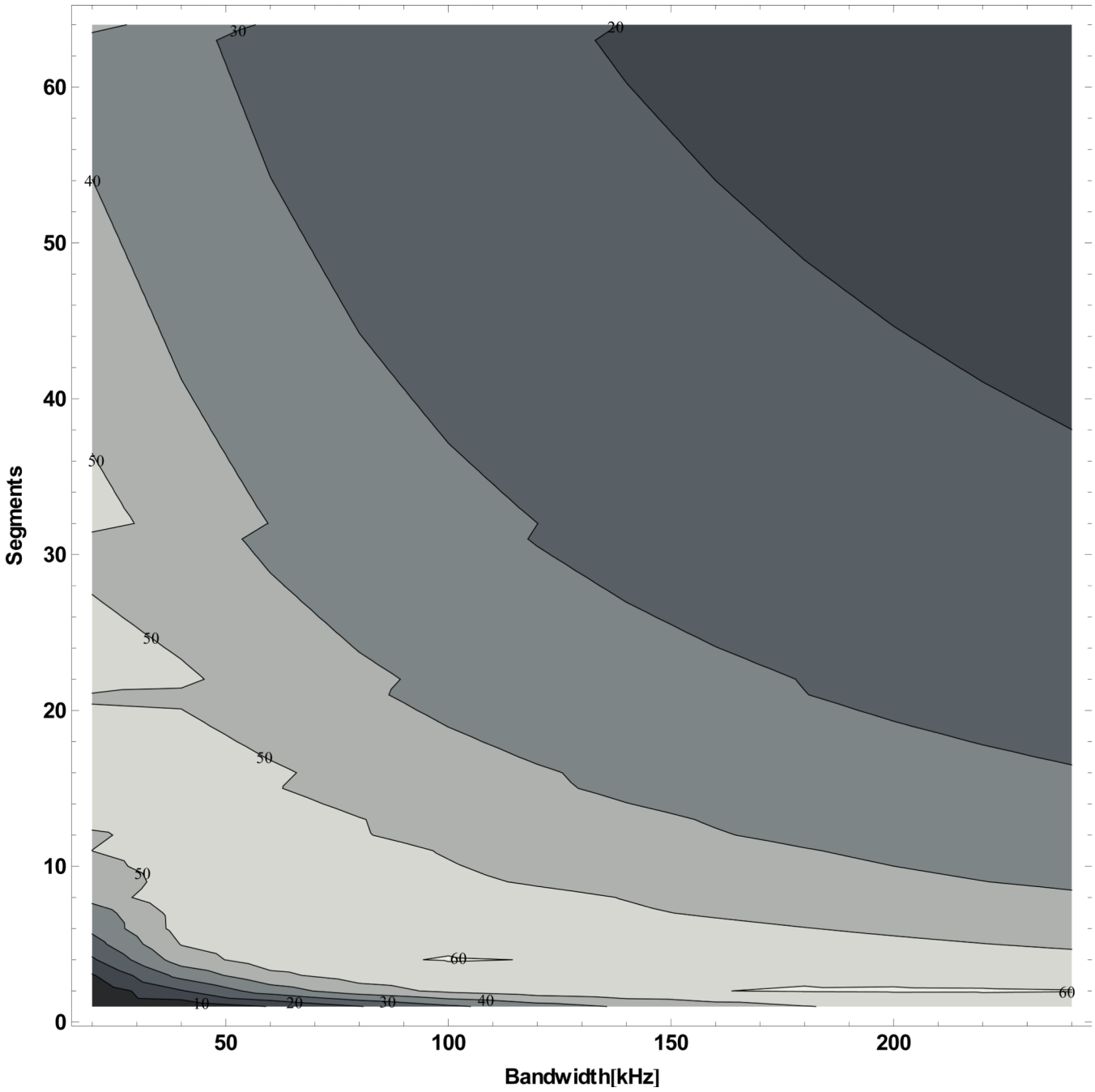

Figure 4.

Contour plot of SNR of the sequence shown in Figure 1 (arbitrary units). The horizontal axis represents acquisition bandwidth in kHz and the vertical axis the number of segments used. See the Materials and Methods section for the remaining parameters used in this numerical simulation.

Table 1

The SNR and FA values from 6 animals, measured in gray matter and white matter regions. The SNR values were obtained from images without diffusion weighting.

	SNR (mean ± SD)	FA (mean ± SD)
Cortex	121 ± 15	0.25 ± 0.02
Corpus Callosum	167 ± 18	0.56 ± 0.04